Electronic Supplementary Material (ESI) for Polymer Chemistry.
This journal is © The Royal Society of Chemistry 2020

Supporting Information

Water-soluble hyperbranched polyglycerol photosensitizer for enhanced photodynamic therapy

Bowen Xiang, ‡[a] Yudong Xue, ‡[a] Zhiyong Liu, [a] Jia Tian, [a] Holger Frey, *[b] Yun Gao, [a] and Weian Zhang, *[a]

[a.] Shanghai Key Laboratory of Functional Materials Chemistry, East China University of Science and Technology, Shanghai 200237, China. E-mail: wazhang@ecust.edu.cn

[b.] Institute of Organic Chemistry, Johannes Gutenberg University, Duesbergweg 10-14, 55128 Mainz, Germany. E-mail: hfrey@uni-mainz.de

Characterizations

^{1}H NMR and ^{19}F NMR spectra were acquired by a Bruker AV400 MHz NMR spectrometer using $CDCl_3$ or DMSO-d_6 with tetramethylsilane (TMS) as an internal reference. Mass spectrum (MS) was recorded on a Waters LCT Premier XE spectrometer with methyl alcohol as the solvent. Transmission electron microscopy (TEM) analysis was performed using a JEOL JEM1400 electron microscope operated at 100 kV. Samples for TEM were prepared by dropping the nanoparticle solution onto a carbon-coated copper grid and then dried at room temperature. The UV-Vis spectra of the samples were measured by a UV-2450 UV-Visible spectrophotometer. Confocal laser scanning microscopy (CLSM) was performed on a Nikon A1R.

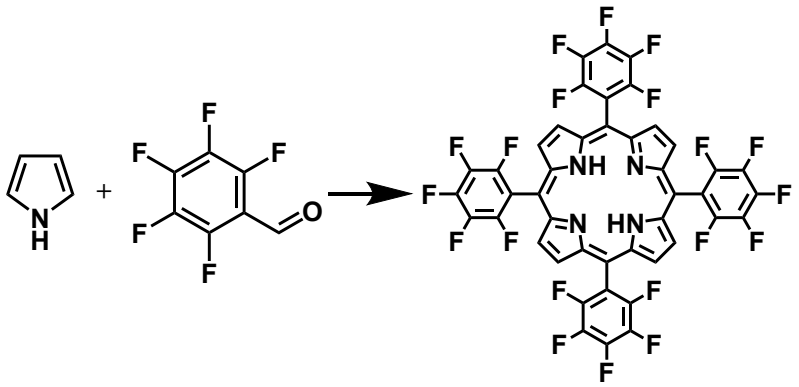

Scheme S1. Schematic illustration for the synthesis of $TF_{20}PP$.

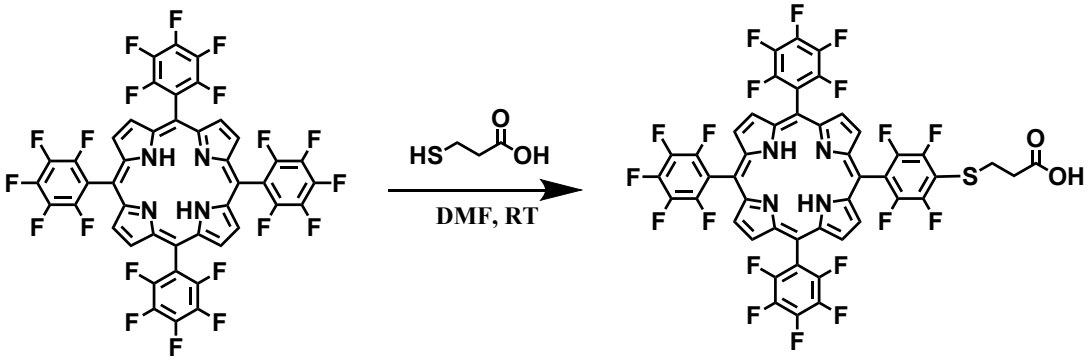

Scheme S2. Schematic illustration for the synthesis of $TF_{19}PP$-COOH.

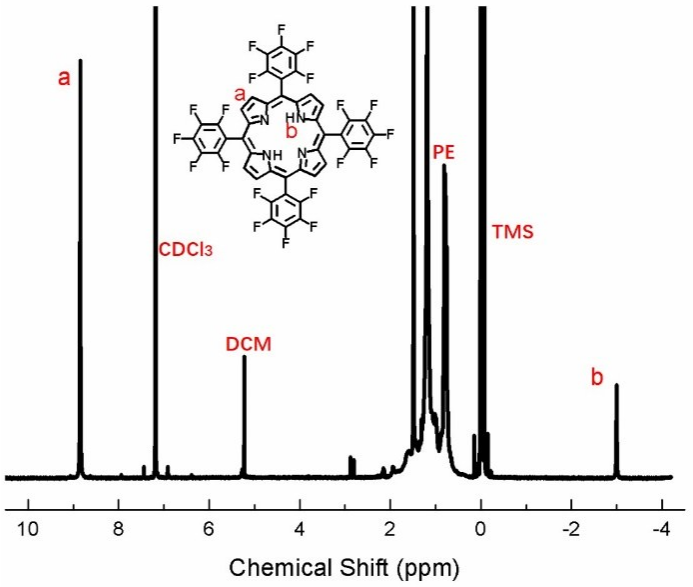

Fig. S1. ^{1}H NMR spectrum of $TF_{20}PP$.

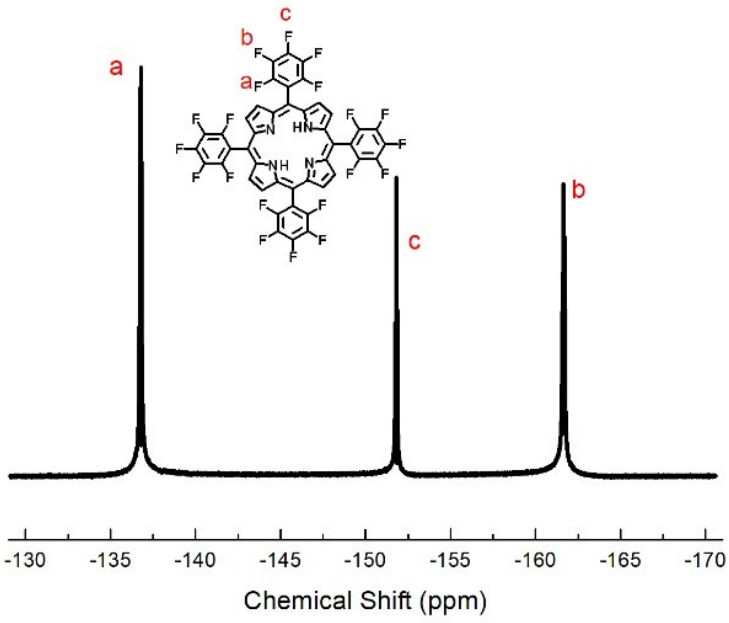

Fig. S2. ^{19}F NMR spectrum of $TF_{20}PP$.

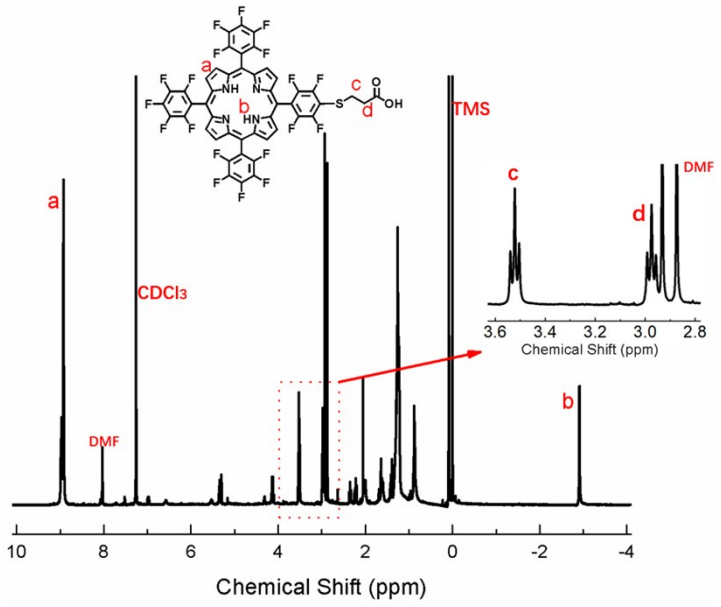

Fig. S3. ^{1}H NMR spectrum of $TF_{19}PP$-COOH.

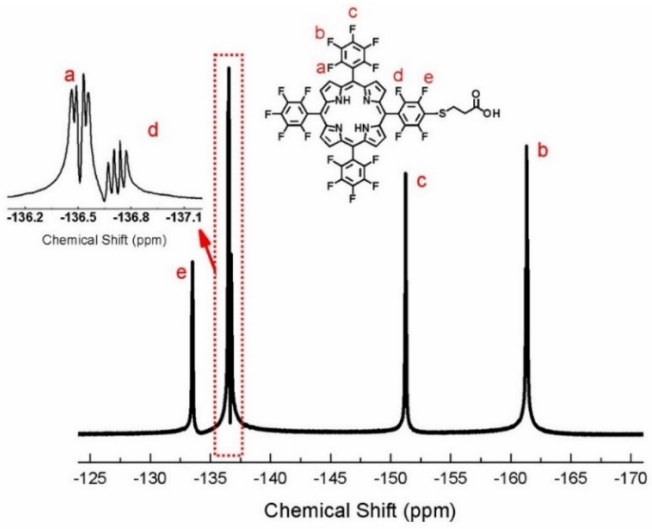

Fig. S4. ^{19}F NMR spectrum of $TF_{19}PP$-COOH.

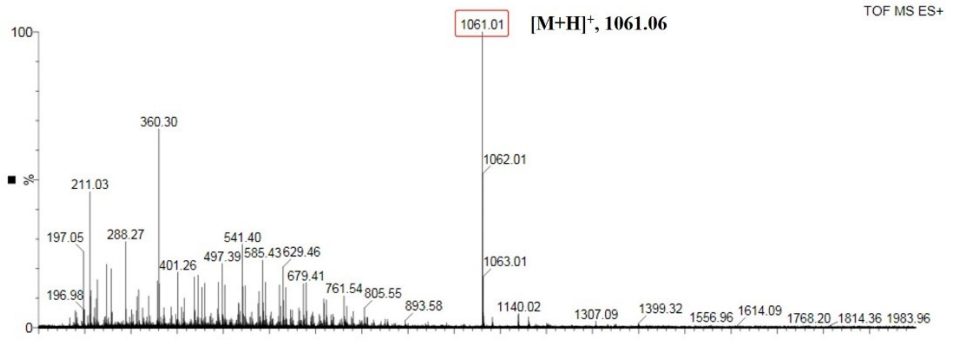

Fig. S5. MS spectrum of $TF_{19}PP$-COOH. MS spectrum of $TF_{19}PP$-COOH. MS (ESI+, 100% CH_3OH): calculated for $C_{47}H_{15}F_{19}N_4O_2S$ [M+H]+, 1061.06, found 1061.01.

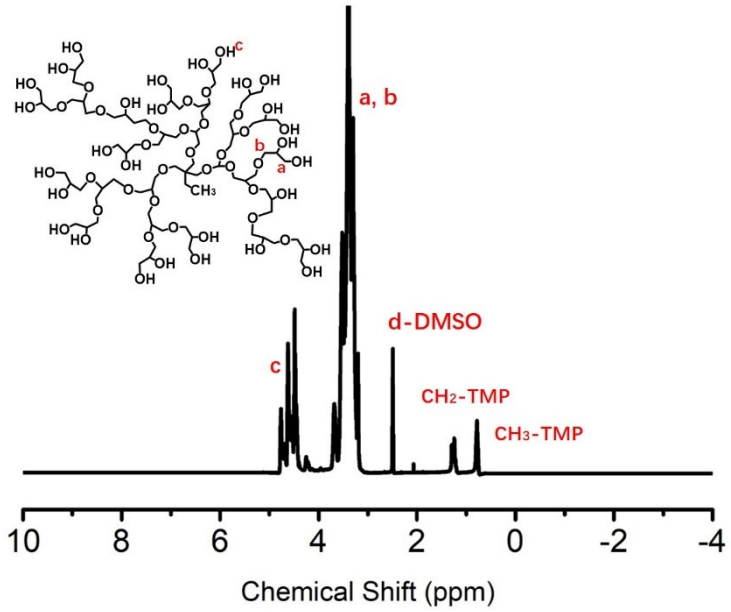

Fig. S6. ^{1}H NMR spectrum of hbPG.

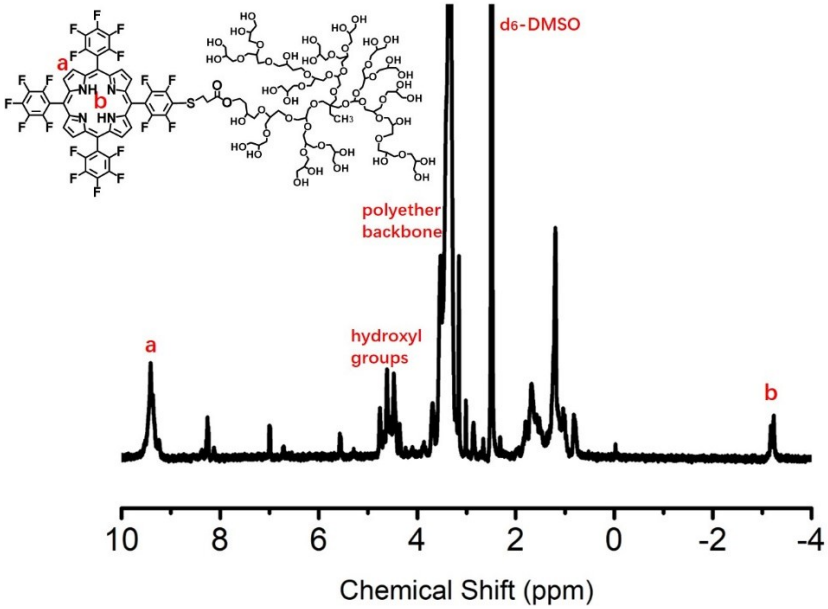

Fig. S7. ^{1}H NMR spectrum of hbPG-FP1.

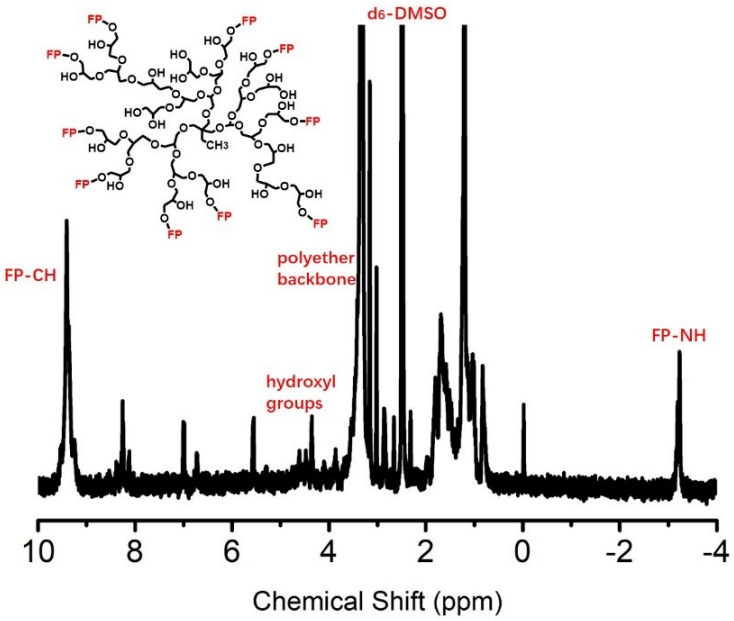

Fig. S8. ^{1}H NMR spectrum of hbPG-FP2.

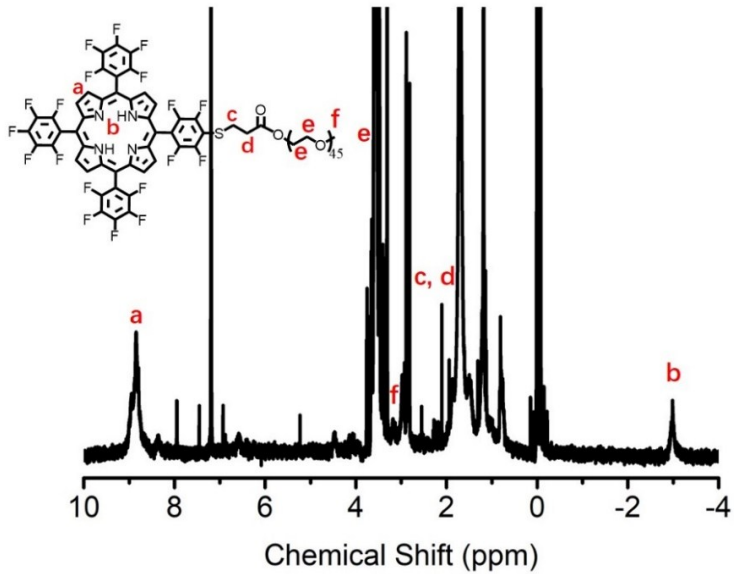

Fig. S9. ^{1}H NMR spectrum of LPEG-FP.

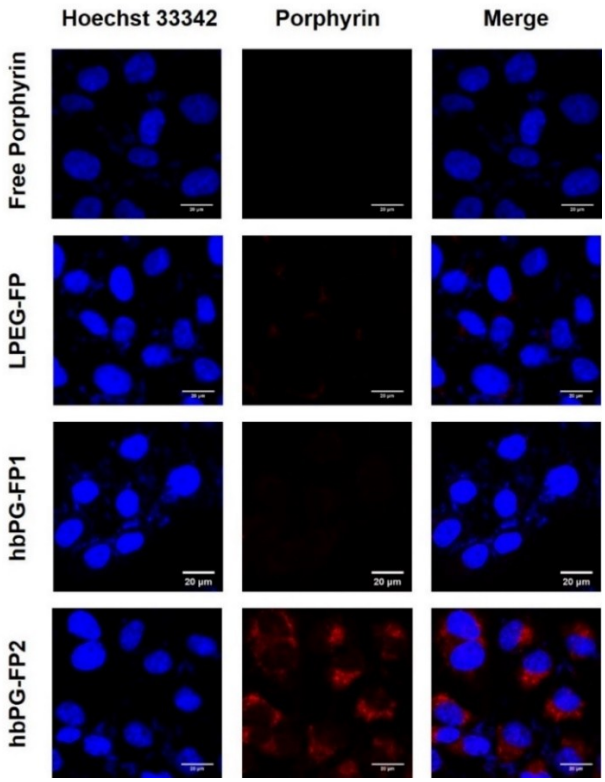

Fig. S10. CLSM images of HeLa cells incubated with free porphyrin ($TF_{20}PP$), LPEG-FP, hbPG-FP1 and hbPG-FP2 nanoparticles for 4 h. The images from left to right are the cells with nuclear staining with Hoechst 33342, those with porphyrin fluorescence and the merge of the images (scale bar: 20 µm).

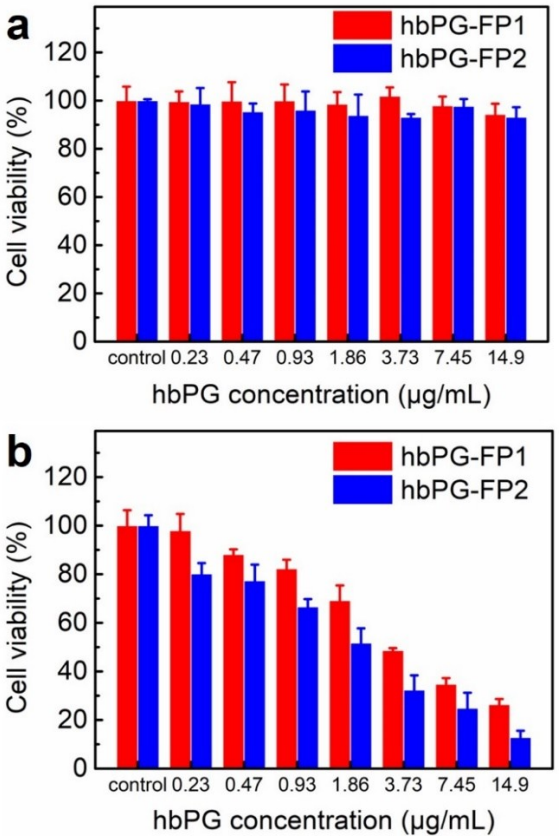

Fig. S11. *In vitro* dark cytotoxicity (a) and phototoxicity (b) of hbPG-FP1 and hbPG-FP2 nanoparticles by MTT assay for Hela cells after incubation with various concentrations of different nanoparticles. The concentration of porphyrin in hbPG-FP1 are 0.125, 0.25, 0.5, 1, 2, 4, 8 μg/mL, respectively. The concentration of porphyrin in hbPG-FP2 are 1.25, 2.5, 5, 10, 20, 40, 80 μg/mL, respectively. Data were expressed as mean ± standard deviation (n = 3).

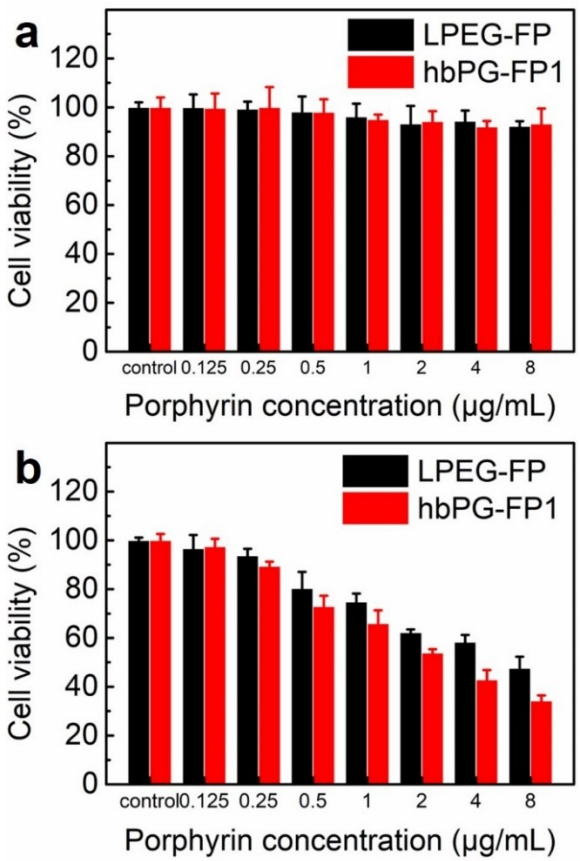

Fig. S12. *In vitro* dark cytotoxicity (a) and phototoxicity (b) of LPEG-FP and hbPG-FP1 nanoparticles by MTT assay for 4T1 cells after incubation with various concentrations of different nanoparticles. Data were expressed as mean ± standard deviation (n = 3).

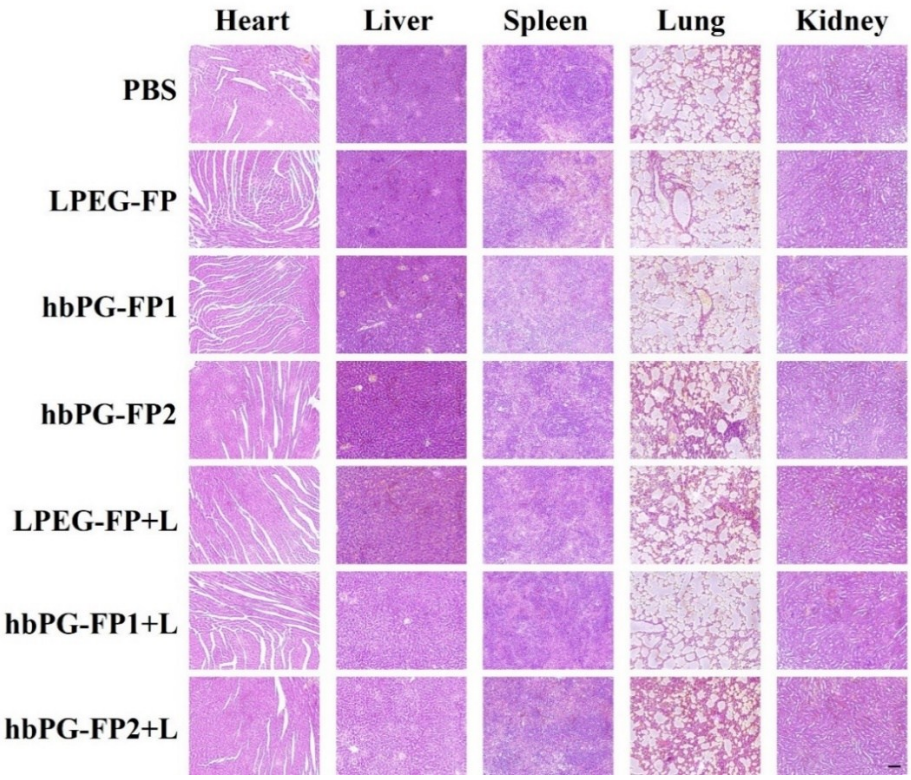

Fig. S13. H&E staining micrographs of main organs (heart, liver, spleen, lung, and kidney) from mice of different groups (scale bar: 100 μm).